Confidence Interval Based Distributionally Robust Real-Time Economic Dispatch Approach Considering Wind Power Accommodation Risk

Li, Peng; Yang, Ming; Wu, Qiuwei

Published in:
IEEE Transactions on Sustainable Energy

Link to article, DOI:
10.1109/TSTE.2020.2978634

Publication date:
2021

Document Version
Peer reviewed version

Citation (APA):
Li, P., Yang, M., & Wu, Q. (2021). Confidence Interval Based Distributionally Robust Real-Time Economic Dispatch Approach Considering Wind Power Accommodation Risk. *IEEE Transactions on Sustainable Energy*, *122*(1), 58 - 69. https://doi.org/10.1109/TSTE.2020.2978634

Confidence Interval Based Distributionally Robust Real-Time Economic Dispatch Approach Considering Wind Power Accommodation Risk

Peng Li, *Student Member, IEEE,* Ming Yang, *Senior Member, IEEE,*
Qiuwei Wu, *Senior Member, IEEE*

***Abstract*—This paper proposes a confidence interval based distributionally robust real-time economic dispatch (CI-DRED) approach, which considers the risk related to accommodating wind power. In this paper, only the wind power curtailment and load shedding due to wind power disturbances are evaluated in the operational risk. The proposed approach can strike a balance between the operational costs and risk even when the wind power probability distribution cannot be precisely estimated. A novel ambiguity set is developed based on the imprecise probability theory, which can be constructed based on the point-wise or family-wise confidence intervals. The worst pair of distributions in the established ambiguity set is then identified, and the original CI-DRED problem is transformed into a determined nonlinear dispatch problem accordingly. By using the sequential convex optimization method and piecewise linear approximation method, the nonlinear dispatch model is reformulated as a mixed integer linear programming problem, for which off-the-shelf solvers are available. A fast inactive constraint filtration method is also applied to further relieve the computational burden. Numerical results on the IEEE 118-bus system and a real 445-bus system verify the effectiveness and efficiency of the proposed approach.**

***Index Terms*—Ambiguity set, confidence interval, distributionally robust, economic dispatch, imprecise probability theory, operational risk.**

NOMENCLATURE

A. Sets and Indices:

$i \in \mathcal{G}$	AGC units.
$m \in \mathcal{M}$	Wind farms.
$l \in \mathcal{L}$	Transmission lines.
$t \in \mathcal{T}$	Time periods.
$j \in \mathcal{J}$	Conventional Loads.

B. Decision Variables:

$p_{i,t}/\alpha_{i,t}$	Base point/participation factor of generators.
$\Delta p_{i,t}^{up}/\Delta p_{i,t}^{dn}$	Upward reserve capacity/downward reserve capacity for generators.
$w_{m,t}^{u}/w_{m,t}^{l}$	Upper/lower output bound of wind farms.
$\Delta p_{m,t}^{up}/\Delta p_{m,t}^{dn}$	Maximum allowed upward/downward disturbance of wind farms m in period t, satisfying $\Delta p_{m,t}^{dn} = p_{m,t} - w_{m,t}^{l}$, $\Delta p_{m,t}^{up} = w_{m,t}^{u} - p_{m,t}$.
$w_{m,t,s'}^{u}/w_{m,t,s'}^{l}$	Value of $w_{m,t}^{u}/w_{m,t}^{l}$ in segment $(s^{'}, s'+1)$.
$U_{m,t,s'}^{u}/U_{m,t,s'}^{l}$	Binary variable indicating whether the actual wind power is located at segment $(s^{'}, s'+1)$.
$\lambda_{ml,t}^{up}/\lambda_{ml,t}^{dn}$	Auxiliary decision variables for transmission capacity constraints.

C. Parameters:

c_i	Price of generators to provide energy.
$\hat{c}_i/\check{c}_i$	Price of generators for providing upward/ downward flexible capacity.
θ^l/θ^u	Prices for the load shedding/the wind power curtailment.
$\phi_{m,t}^{PS}/\phi_{m,t}^{WP}$	Operational risk related to the load shedding/ the wind power curtailment.
w_m^{max}	Installed capacity of wind farms.
$p_{m,t}$	Expected output of wind farms.
$d_{j,t}$	Load demand of load node j.
D_t	Amount of the load demand, which is pre-specified.
$M_{il}/M_{ml}/M_{jl}$	Generation shift distribution factors of generators/wind farms/loads.
$G/M/T/L$	Number of AGC units/wind farms/time periods/ transmission lines.
p_i^{max}/p_i^{min}	Maximal/minimal output of generators.
R_i^{up}/R_i^{dn}	Ramp-up/ramp-down limitation for generators.
T_l	Transmission capacity of lines.
$o_{m,t,s'}^{u}/o_{m,t,s'}^{l}$	Break points of the upward/downward wind power disturbance region.
x	Output of wind farms.
$\underline{P}(x)/\overline{P}(x)$	Confidence bands of the cumulative distribution function of random variable x.
$F_x(X)$	Probability of the random event $x \leq X$.

D. Random Variables:

$\tilde{p}_{m,t}$	Random outputs of wind farms.
$\Delta\tilde{p}_{i,t}$	Random reserve of AGC generators.
$\Delta\tilde{p}_{m,t}$	Random disturbances of wind farms.

Manuscript received March 19, 2019; revised September 4, 2019 and December 29, 2019; accepted February 29, 2020. This work was supported in part by the Shandong Provincial National Science Foundation of China under Grant ZR2018MEE041, and in part by the Science and Technology Project of State Grid Corporation of China under Grant 52060018000X. Paper no. TSTE-00318-2019. *(Corresponding author: Ming Yang.)*

P. Li, and M. Yang are with the Key Laboratory of Power System Intelligent Dispatch and Control, Shandong University, Jinan 250061, China (e-mail: pengli121121@yahoo.com; myang@sdu.edu.cn).

Q. Wu is with the Center for Electric Power and Energy (CEE), Department of Electrical Engineering, Technical University of Denmark (DTU), Kgs. Lyngby 2800, Denmark, and also with the School of Electrical Engineering, Shandong University, Jinan 260061, China (e-mail: qw@elektro.dtu.dk).

Color versions of one or more of the figures in this article are available online at https://ieeexplore.ieee.org.

Digtial Object Identifier

I. Introduction

ECONOMIC dispatch (ED) is fundamental in power system operation, which aims to allocate the forecasted load among committed generators at minimum total cost, while satisfying all concerned operational constraints [1]–[3]. Over the past decades, as a solution of the global crisis in energy resources and environment, large-scale renewable energy has been widely integrated into power systems, which significantly intensifies the uncertainty in power system operation, and thus poses huge challenges on conventional ED methods.

To meet these challenges, great efforts have been devoted to improving the current ED practice so that more renewable energy can be accommodated at a reasonable cost. For example, a stochastic ED model for real-time power system operation was formulated in [4], where the concept of uncertainty responses is introduced to assess the power system operational risk with respect to net load uncertainties. Ref. [5] investigated a multi-objective stochastic ED model considering wind power integration, which is transformed into an equivalent deterministic optimization problem based on the scenario method. A stochastic programming (SP) framework for multiple timescale ED that can enhance the renewable energy integration was presented in [6]. The framework allows slow-response and fast-response energy resources to be controlled at different timescales. However, the effectiveness of the SP-based methods depends on the quality of the probability distribution function (PDF), which cannot be guaranteed in practice.

Another tool for optimization in the presence of uncertainties is robust optimization (RO), which is more efficient than SP in general [7]. RO minimizes the worst-case cost over all possible realizations within a deterministic uncertainty set, ignoring the probability information [8]. Many RO-based ED methods have been investigated in the literature, in which the adopted uncertainty sets are usually predetermined [9]–[11], and thus over-conservative decisions may be obtained. To overcome this shortcoming, several studies utilize dynamic confidence levels to develop an adjustable uncertainty set [12]. Furthermore, [13] incorporated the probability distribution function (PDF) of wind power into robust ED problems. However, like the SP-based methods, the RO-based methods that consider the PDFs of wind power also rely on the precisely known PDFs, which restricts the practicability of the methods.

Recently, distributionally robust optimization (DRO), which assumes that the true distribution of uncertainties lies in an ambiguity set, is proposed to address the above issues. One of the most popular DRO approaches is the moment-based DRO, where the ambiguity sets are constructed using all probability distributions with given mean and covariance. In [14], a moment-based DRO model was presented for the reserve schedule problem with partial wind power information, i.e., the PDF of wind power is unknown while its statistical moments are available. Ref. [15] proposed a moment-based DRO model for the co-ordinated reserve scheduling problem, considering the operational risk. In [16], a two-stage moment-based DRO model for the joint energy and reserve dispatch of power systems was proposed. Ref. [17] proposed a new moment-based DRO model for power system ED problems. However, the PDF or cumulative distribution function (CDF) contains more information than the moments, and is not fully utilized in the moment-based DRO, which may lead to over-conservative decisions [18]. Meanwhile, the moment-based DRO problems are usually formulated as a semidefinite programming (SDP), which is very computationally intensive. Besides, the moments estimated from sample data may also be uncertain. To address the issues, some distance-based DRO methods are proposed, which believe that the true distribution is not far away from the empirical distribution. In the distance-based DRO methods, the ambiguity set is a family of probability distributions within a fixed distance from the empirical distributions. The distance between two distributions can be measured by the KL divergence or the Wasserstein metric, resulting in KL-divergence-based DRO approaches or Wasserstein-metric-based DRO approaches. Ref. [18] proposed a distance-based distributionally robust unit commitment model via the KL divergence, where the ambiguity set is a family of distributions within a fixed distance from an empirical distribution. However, the KL-divergence-based DRO cannot be applied to stochastic optimization models with heavy tail random functions due to infinite worst-case expectation. Moreover, to estimate KL-divergence-based ambiguity sets, each training sample must be assigned positive probability mass. Ref. [19] discussed a distributionally robust chance constrained approximate AC optimal power flow (OPF), where the ambiguity set is the Wasserstein ball centered at the empirical distribution. In [20], the similar Wasserstein-metric-based ambiguity set was employed to establish a new DRO model for the risk-based ED problem. Ref. [21] proposed a risk-based DRO approach to investigate the OPF with dynamic line rating, considering a new distributional uncertainty set based on the moment and the Wasserstein metric. The Wasserstein-metric-based DRO approaches can overcome the shortcomings of the KL-divergence-based DRO approaches, but as mentioned in [21], they are usually difficult to solve and their computational burden grows heavily with the amount of the data employed to construct the ambiguity set. Besides, in [18] and [19], the risk costs of accommodating wind power were ignored and the admissible region of wind power (ARWP) cannot be obtained from the optimization results directly. In [20], the ARWP has to be centered at the expected wind power output, which may lead to sub-optimal decisions.

The concept of the operational risk resulting from uncertainties is also introduced in power system operation optimization problems. In [22], a risk-based OPF model was proposed, where a trade-off between the generation costs and the conditional energy transaction costs is made based on the conditional value-at-risk method, neglecting the operational risk related to wind power curtailment. Ref. [23] proposed a risk-based ED model to determine the optimal spinning reserve capacity based on the conditional value-at-risk method, where a predetermined confidence level is required to calculate the conditional value-at-risk. However, in practice, selecting a suitable confidence level is lack of systematic methods. In [24], a novel risk-based day-ahead unit commitment model was presented, where the risks of the loss of load, wind curtailment and branch overflow caused by wind

power uncertainty are considered. A robust risk-constrained unit commitment formulation was also proposed in [25] to cope with large-scale volatile and uncertain wind generation. Each of the aforementioned risk-based models has its own merits. However, on the one hand, they usually rely heavily on the exact PDF of wind power, which is hard to be estimated precisely in practice. In other words, the uncertainties of wind power distributions are ignored in these risk-based models. And thus, the risk reliability will not be guaranteed. On the other hand, the ARWP on each node cannot be obtained from the optimization results directly in the aforementioned risk-based models.

In this paper, a novel confidence interval (CI) based wind power ambiguity set is constructed based on the imprecise probability theory [26], which generalizes the classical probability theory to allow for partial probability specifications. Then, a confidence interval based distributionally robust real-time economic dispatch (CI-DRED) model is proposed to strike a balance between the operational costs and risk under the worst pair of distributions in the proposed ambiguity set. In the proposed model, only the wind power curtailment and load shedding due to wind power disturbances are evaluated in the operational risk. According to the proposed model, an optimal ARWP on each node can be obtained. By using the sequential convex optimization method and piecewise linear approximation method, the CI-DRED model is converted into a mixed integer linear programming (MILP) problem. Moreover, a fast inactive constraint filtration method is also applied to further relieve the computational burden. The advantages of the proposed approach are as follows.

i) A CI-DRED model is proposed based on the RO architecture, which can provide explicit operational risk reliability guarantee to ensure the risk robustness of economical system operation. And the optimal admissible region of wind power for each wind farm can also be obtained from the solution directly, providing important information for wind farms.
ii) A novel CI-based ambiguity set is proposed, which can be constructed from available observations directly without any prior knowledge about the distribution. The more samples are available, the less conservative solution is obtained. Compared with the moment-based ambiguity sets, more information is included in the proposed ambiguity set, and thus less conservative decisions can be obtained. Compared with the distance-based ambiguity sets, the scale of the proposed model remains unchanged as the available data increases and the proposed ambiguity set can be applied to any type of distributions.
iii) An efficient algorithm incorporating the risk estimation method, sequential convex optimization method, and inactive constraint filtration method is proposed to transform the proposed model into a mixed integer linear programming (MILP), significantly reducing the computational burden and making the proposed approach suitable for large-scale power system applications.

The remaining parts of this paper is organized as follows. In Section II, the wind power ambiguity set is constructed and the operational risk is introduced. Section III describes the mathematical formulation of CI-DRED. In Section IV, the solution methodology is presented. Case studies are reported in Section V and the conclusions are drawn in Section VI.

II. Risk Considering Distributional Uncertainty

A. Wind Power Ambiguity Set

In many cases, the wind power PDF cannot be estimated precisely due to insufficient information. To address this issue, all possible distributions should be considered in the optimization to make a distributionally robust decision, and the set that contains all these distributions is referred to as an ambiguity set [16]. Different from the moment-based ambiguity set [14], a novel CI-based ambiguity set is constructed using the confidence interval-based ambiguity set construction method (CIAS). CIAS can directly establish the confidence bands (CBs) for the CDF of wind power. All probability distributions, whose CDFs are within the CBs, construct the proposed ambiguity set.

As is well known, the CDF of a real-valued random variable x can be defined as $F_x(X) = P(x \leq X)$, indicating the probability of the random event $x \leq X$. Specifically, if we have a out of b independent and identically distributed samples less than or equal to A and $b \to +\infty$, the probability $F_x(A)$ will be a/b according to the Law of Large Numbers. By repeating this process for all points in the support of x, we can obtain the CDF of x (See Fig. 1(a)). However, in practice, only finite samples of x are available, e.g., wind power, which violates the Law of Large Numbers. In this case, the preciseness of the probability estimated for $x \leq X$ cannot be assured and thus the obtained CDF will be unreliable. To indicate the uncertainty existing in the estimated CDF, the CBs of the CDF are explicitly estimated with respect to the available data.

According to the definition of CDF, three key steps are designed to estimate the CBs of wind power CDF.

1) **(Confidence intervals for sample points)** Given a sample set of the random wind power x, for each sample point of x, say A, the CI of the probability of $x \leq A$ at a specified confidence level is estimated, as shown in Fig. 1(a). By this step, the upper and lower bounds of the random wind power CDF at each sample point can be obtained, as shown in Fig. 1(b).
2) **(Confidence intervals for points that are not sample points)** Since only finite samples are available in practice, in Step 1), CIs are just calculated at the sample points. However, because the wind power CDF is non-decreasing, the confidence intervals at the points that are not the sample points can then be safely estimated using the interpolation methods. For example, we have two adjacent sample points, i.e., X_k and X_{k+1}, as shown in Fig. 1(c). For any point within these two sample points, its cumulative probability confidence intervals can be safely estimated as $[a_k, b_{k+1}]$, where a_k and b_{k+1} are the lower bound of cumulative probability confidence interval at sample point X_k and the upper bound of cumulative probability confidence interval

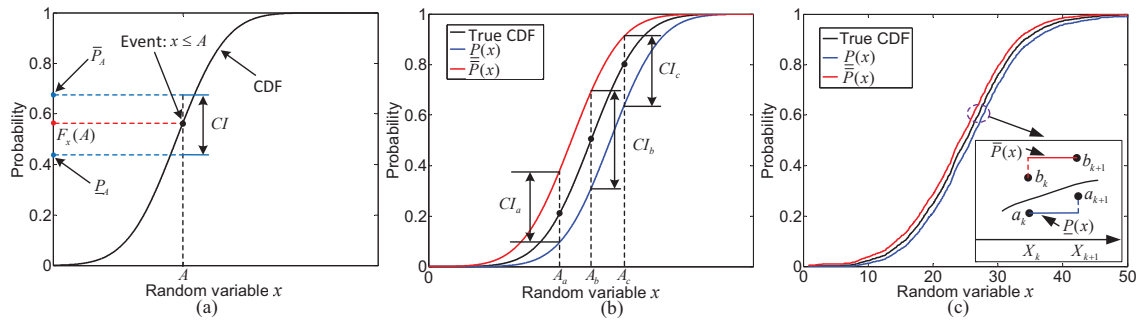

Fig. 1. Diagrams of (a) the CI at one sample point over the CDF, (b) constructing the CBs of the CDF, and (c) the stair-step interpolation method.

at sample point X_{k+1}, respectively. By this step, the confidence intervals of the wind power cumulative probability at each point that is not sample point can be obtained.

3) **(Conference bounds for the whole CDF)** By connecting the lower and upper bounds of the confidence intervals obtained in Step 1) and Step 2), respectively, the confidence bands of the wind power whole CDF are constructed, as shown in Fig. 1(c).

In this paper, the CI at each sample point is estimated based on the imprecise probability theory, which is a generalization of the classical probability theory allowing partial probability specifications. Typically, it quantifies the uncertainty of a random event by a probability interval (PI) [26]. For instance, the imprecise probabilities of $x \le A$ and its complementary event $x > A$ can be expressed by $\tilde{P}_A = [\underline{P}_A, \overline{P}_A]$ and $\tilde{P}_{\bar{A}} = [\underline{P}_{\bar{A}}, \overline{P}_{\bar{A}}]$, satisfying $\underline{P}_A + \overline{P}_{\bar{A}} = 1$, $\overline{P}_A + \underline{P}_{\bar{A}} = 1$, $0 \le \underline{P}_A \le \overline{P}_A \le 1$, and $0 \le \underline{P}_{\bar{A}} \le \overline{P}_{\bar{A}} \le 1$. The width of the estimated PI is closely related to the historical data. The more the historical data, the narrower the PI. If sufficient data are available, the interval may shrink to a single point and a precise probability will be obtained [27].

In this paper, CIAS applies the method in [28] and [29], which can estimate the PI according to a specified confidence level, i.e., γ, to estimate the CIs. Specifically, the γ-CI of $F_x(A) = P(x \le A)$ can be estimated by

$$\begin{cases} a_k = 0, \quad b_k = G^{-1}(\frac{1+\gamma}{2}), & n_k = 0, \\ a_k = H^{-1}(\frac{1-\gamma}{2}), \quad b_k = G^{-1}(\frac{1+\gamma}{2}), & 0<n_k<n, \\ a_k = H^{-1}(\frac{1-\gamma}{2}), \quad b_k = 1, & n_k = n, \end{cases} \tag{1}$$

where a_k and b_k are the lower and upper bounds of the CI, respectively, H is the CDF of beta distribution $B(n_k, s+n-n_k)$, G is the CDF of beta distribution $B(s+n_k, n-n_k)$, n_k is the number of the samples satisfying $x \le A$, n is the sample size, and s is the equivalent sample size [29]. By this means, the CI at each sample point can be obtained.

For the second step, a simple stair-step interpolation is applied to obtain the CBs of the whole CDF [30], which can be expressed as (2), as shown in Fig. 1(c).

$$\begin{cases} \underline{P}(x) = a_k, & x \in (X_k, X_{k+1}], \\ \overline{P}(x) = b_{k+1}, & x \in [X_k, X_{k+1}). \end{cases} \tag{2}$$

Finally, the ambiguity set $\mathcal{A}$ can be constructed as

$$\mathcal{A} = \{F_x | F_x(X) \in [\underline{P}(X), \overline{P}(X)]\}. \tag{3}$$

Remark 1: Note that the spatial correlation of probability distributions of multiple wind power plant random outputs is not exploited in the ambiguity set. It should be pointed out that this treatment inevitably brings additional conservatism to the obtained decisions. However, this treatment also possesses the following advantages: 1) Tractability: The optimization models ignoring the spatial correlation of probability distributions of multiple wind power plant random outputs can usually be transformed into tractable convex problems whereas those incorporated the spatial correlation usually form non-convex problems, which cannot be effectively solved by off-the shelf solvers. 2) Scalability: Based on this treatment, the dimension of the constructed ambiguity set grows linearly with the number of wind power plants, which can contribute to the highly scalable algorithm. Nevertheless, when the spatial correlation is considered in the ambiguity set, the dimension of the ambiguity set will increase much faster with the number of wind power plants compared with this treatment, which will significantly increase the computational complexity. Specifically, the dimension of the ambiguity set that ignores the spatial correlation is $N' \times 1$ where as the dimension of the ambiguity set that considers the spatial correlation is $N' \times N'$, where N' is the number of wind power plants. Of course, since the spatial correlation has a significant impact on the overall wind power uncertainty, a practical and computational efficient model considering the spatial correlation would be one of our future research directions.

B. PW Confidence Intervals and FW Confidence Intervals

It should be pointed out that besides the CI obtained using the approach presented in this paper (hereafter referred to as PW-CI), there is another kind of CI, named as the FW-CIs, which can be estimated by the Calibration for Simultaneity-based method in [30]. In fact, the CIAS method can also be used to estimate the FW-CIs. It only needs to adjust some parameters and conditions in the CIAS. Then, the FW-CI can be obtained by estimating the particular PW-CI.

Compared with the FW-CI obtained using the method mentioned in [30], the PW-CI obtained using the approach presented in this paper has the following three significant differences:

- In the method in [30], only a uniform distribution is used as the prior distribution. In contrast, to avoid the prejudice of the prior distribution, the approach presented in this

paper uses a set of prior distributions instead of a single prior distribution, which will result in more robust bound estimations for PW-CIs.

- To estimate PW-CIs, the parameter s is used to tune the influence of the prior distribution on the posterior distribution. The larger the value of s, the more significant the influence. In contrast, to estimate FW-CIs, a fixed parameter, i.e., $s = 1$, is adopted, which is a particular case of PW-CIs.
- To estimate FW-CIs, the employed samples of random variables have to be different from each other, which may not take full advantage of all available samples in practice. In contrast, to estimate PW-CIs, all available samples can be made full use of, regardless of whether there are identical samples in the available sample set.

Therefore, PW-CIs are more general compared with FW-CIs obtained using the method mentioned in [30] and thus the PW-CIs are recommended for constructing the ambiguity set in this paper.

C. Wind Power Accommodation Risk

The wind power disturbances within the ARWP can be accommodated by the system safely. Otherwise, undesired power imbalance that cannot be fully handled by the committed units themselves may occur [13]. In such a situation, additional emergency regulations, i.e, load shedding or wind generation curtailment in this paper, may have to be used to recover the operational security [25]. Therefore, in this paper, considering the distributionally uncertainty, the worst expected cost for such emergency regulations is referred to as operational risk that can be taken as the economic loss in operation. Fig. 2 provides a diagram of operational risk under the CDF of wind power. In the figure, $F_a(x)$ and $F_b(x)$ are the CBs of the wind power CDF; w^l and w^u mean the lower and upper bounds of the admissible region. For the given node, if actual wind power x is within the admissible region $[w^l,w^u]$, the wind power can be accommodated by the system safely. In this case, no additional emergency regulations are required and thus no economic loss is caused by wind power disturbances. If the actual wind power is greater than the upper bound of the admissible region, i.e., $x>w^u$, the wind power has to be curtailed to ensure system operational security. Similarly, if the actual wind power is less than the lower bound of the admissible region, i.e., $x<w^l$, a load shedding will be required. Thus, the total operational risk of the node is the economic loss due to wind power curtailment and load shedding. And the system operational risk can be obtained by summing all the nodal operational risk.

Accordingly, the operational risk of wind power curtailment and load shedding at a given node can be computed by

$$\begin{aligned}\max_{P_m\in\mathcal{A}_m}\phi_{m,t}^{PS} &= \max_{P_m\in\mathcal{A}_m} E_{P_m}[\left(w_{m,t}^l - x\right)|0 \le w_{m,t}^l - x \le w_{m,t}^l] \\ &= \max_{P_m\in\mathcal{A}_m}\int_0^{w_{m,t}^l}(w_{m,t}^l - x)P_m(x)dx, \end{aligned} \tag{4}$$

$$\begin{aligned}\max_{P_m\in\mathcal{A}_m}\phi_{m,t}^{WP} &= \max_{P_m\in\mathcal{A}_m} E_{P_m}[\left(x - w_{m,t}^u\right)|w_{m,t}^u \le x \le w^{max}] \\ &= \max_{P_m\in\mathcal{A}_m}\int_{w_{m,t}^u}^{w^{max}}(x - w_{m,t}^u)P_m(x)dx, \end{aligned} \tag{5}$$

where $P_m(x)$ is the PDF of wind power x, which is one of the probability distributions in the ambiguity set $\mathcal{A}_m$; Eq. (4) and Eq. (5) indicate the expected loss for loading shedding and wind power curtailment under the worst distribution in the ambiguity set $\mathcal{A}_m$, respectively.

Moreover, according to the partial integration method, $\phi_{m,t}^{PS}$ can be reformulated as

$$\begin{aligned}\phi_{m,t}^{PS} &= \left\{(w_{m,t}^l - x)F_m(x)\Big|_0^{w_{m,t}^l} + \int_0^{w_{m,t}^l}F_m(x)dx\right\} \\ &= \int_0^{w_{m,t}^l}F_m(x)dx, \end{aligned} \tag{6}$$

where $F_m(x)$ is the CDF of x. Similarly, $\phi_{m,t}^{WP}$ can be reformulated as

$$\phi_{m,t}^{WP} = w^{max} - w_{m,t}^u - \int_{w_{m,t}^u}^{w^{max}}F_m(x)dx, \tag{7}$$

Then, for a given power system node, its operational risk can be estimated by Eq. (4)-Eq. (7).

III. Optimization Model

CI-DRED aims to minimize the total cost, including the operational costs and risk costs. Without loss of generality, it is assumed that only AGC units are schedulable in ED to simplify the symbolic representation. Thus, CI-DRED can be modeled as follows.

$$\begin{aligned} z = \min\sum_{t\in\mathcal{T}}\Bigg(&\sum_{i\in\mathcal{G}}(c_ip_{i,t} + \hat{c}_i\Delta p_{i,t}^{up} + \check{c}_i\Delta p_{i,t}^{dn}) \\ &+ \sum_{m\in\mathcal{M}}\max_{P_m\in\mathcal{A}_m}(\theta^u\phi_{m,t}^{WP} + \theta^l\phi_{m,t}^{PS})\Bigg), \end{aligned} \tag{8}$$

$$s.t. \qquad (4)-(7),$$

$$\sum_{i\in\mathcal{G}}p_{i,t} + \sum_{m\in\mathcal{M}}p_{m,t} = \sum_{j\in\mathcal{J}}d_{j,t} = D_t, \forall t, \tag{9}$$

$$\sum_{t\in\mathcal{T}}\sum_{m\in\mathcal{M}}\max_{P_m\in\mathcal{A}_m}(\theta^u\phi_{m,t}^{WP} + \theta^l\phi_{m,t}^{PS}) \le Risk_{lim}, \tag{10}$$

$$\Delta p_{i,t}^{up} \ge \alpha_{i,t}\sum_{m\in\mathcal{M}}\Delta p_{m,t}^{dn}, \forall i, \forall t, \tag{11}$$

$$\Delta p_{i,t}^{dn} \ge \alpha_{i,t}\sum_{m\in\mathcal{M}}\Delta p_{m,t}^{up}, \forall i, \forall t, \tag{12}$$

$$\sum_{i\in\mathcal{G}}\alpha_{i,t} = 1, \forall t, \tag{13}$$

$$p_{i,t+1} - p_{i,t} + \Delta p_{i,t}^{dn} + \Delta p_{i,t+1}^{up} \le R_i^{up}, \forall i, \forall t, \tag{14}$$

$$p_{i,t} - p_{i,t+1} + \Delta p_{i,t}^{up} + \Delta p_{i,t+1}^{dn} \le R_i^{dn}, \forall i, \forall t, \tag{15}$$

$$p_i^{min} + \Delta p_{i,t}^{dn} \leq p_{i,t} \leq p_i^{max} - \Delta p_{i,t}^{up}, \forall i, \forall t, \tag{16}$$

$$\sum_{m\in\mathcal{M}} M_{ml}(p_{m,t} + \Delta\tilde{p}_{m,t}) + \sum_{i\in\mathcal{G}} M_{il}(p_{i,t} + \Delta\tilde{p}_{i,t}) + \sum_{j\in\mathcal{J}} M_{jl} d_{j,t} \geq -T_l, \forall l, \forall t, \tag{17}$$

$$\sum_{m\in\mathcal{M}} M_{ml}(p_{m,t} + \Delta\tilde{p}_{m,t}) + \sum_{i\in\mathcal{G}} M_{il}(p_{i,t} + \Delta\tilde{p}_{i,t}) + \sum_{j\in\mathcal{J}} M_{jl} d_{j,t} \leq T_l, \forall l, \forall t, \tag{18}$$

In this problem, the objective function (8) is employed to strike a balance between the operational costs and risk, where the first three terms denote the operational costs, including the generation costs and reserve capacity supply costs, and the last two terms represent the operational risk costs. Eq. (9) describes the power balance requirement in the base case. Eq. (10) denotes the operational risk cost limitation requirement. Eqs. (11)-(12) are the reserve capacity requirements for each AGC unit, where $\Delta p_{m,t}^{dn}$ and $\Delta p_{m,t}^{dn}$ are the maximum allowed downward and upward disturbances of wind power, satisfying $\Delta p_{m,t}^{dn} = p_{m,t} - w_{m,t}^l$, $\Delta p_{m,t}^{up} = w_{m,t}^u - p_{m,t}$. Eq. (13) indicates the sum of all PFs should be equal to 1. Eqs. (14)-(15) are the ramping rate limits of the AGC units, ensuring adequate response capabilities are available even in the worst case. Eq. (16) indicates the generation capacity constraints of the AGC units. Eqs. (17)-(18) are the transmission line power flow limits [11], which are constructed using the shift distribution factors. Random variable $\Delta\tilde{p}_{i,t}$ is the reserve capacity released by AGC unit i. Random variable $\Delta\tilde{w}_{m,t}$ is the disturbance of wind farm m. The total disturbances of wind farms is allocated to the AGC units according to the affine function: $\Delta\tilde{p}_{i,t} = \alpha_{i,t}\sum_{m=1}^{M} \Delta\tilde{p}_{m,t}$.

The objective function (8) and constraints (4)-(7), (9)-(18) form a nonlinear DRO problem with uncertain variables, where $p_{i,t}$, $\alpha_{i,t}$, $w_{m,t}^l$ and $w_{m,t}^u$ are decision variables. The solution methodology will be explained in the next section.

IV. Solution Methodology

Here, we propose an efficient algorithm incorporating the risk estimation method, Soyster's method, sequential convex optimization method, and inactive constraint filtration method. In the risk estimation method, two steps, i.e., deterministic reformulation of risk estimation and linearization of the operation risk, are included. Soysters method is used to equivalently reformulate uncertain constraints as deterministic constraints. The bilinear constraints in the proposed model are handled by the sequential convex optimization method. And the inactive constraint filtration method is employed to improve the computing efficiency by ruling out the inactive constraints. Fig. 3 provide the flowchart of the proposed approach.

A. Deterministic Reformulation of Risk Estimation

By interchanging the maximum and summation, Eq. (19) provides an upper bound on the operational risk estimation.

$$\sum_{t\in\mathcal{T}} \sum_{m\in\mathcal{M}} \left(\max_{P_{m_1}\in\mathcal{A}} \theta^u \phi_{m,t}^{WP} + \max_{P_{m_2}\in\mathcal{A}} \theta^l \phi_{m,t}^{PS} \right) \tag{19}$$

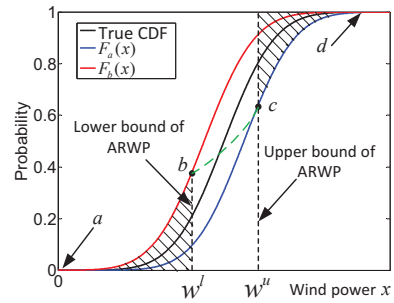

Fig. 2. Diagram of operational risk, copied from [31].

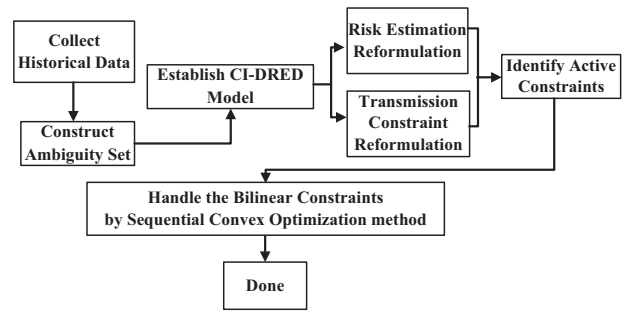

Fig. 3. Flowchart of the proposed approach.

As shown in Fig. 2, the value of $\phi_{m,t}^{PS} = \int_0^{w_{m,t}^l} F_m(x)dx$ equals to the area between $F_m(x)$ and the horizontal axis over $[0, w_{m,t}^l]$. Obviously, for any $F_m(x) \in \mathcal{A}_m$, when $F_m(x) = F_{m,b}(x)$, the area reaches the maximum value. In other words, for $\phi_{m,t}^{PS}$, the worst-case CDF in the ambiguity set (3) is $F_{m,b}(x)$. Therefore, the second term in (19) can be simplified to

$$\sum_{t\in\mathcal{T}} \sum_{m\in\mathcal{M}} \max_{P_m\in\mathcal{A}_m} \phi_{m,t}^{PS} = \sum_{t\in\mathcal{T}} \sum_{m\in\mathcal{M}} \int_0^{w_{m,t}^l} F_{m,b}(x)dx. \tag{20}$$

Similarly, for $\phi_{m,t}^{WP}$, the worst-case CDF in the ambiguity set (3) is $F_{m,a}(x)$. Thus, the first term in (19) can be simplified to the following equation (21).

$$\sum_{t\in\mathcal{T}} \sum_{m\in\mathcal{M}} \max_{P_m\in\mathcal{A}_m} \phi_{m,t}^{WP} = \sum_{t\in\mathcal{T}} \sum_{m\in\mathcal{M}} \left(w^{max} - w_{m,t}^u - \int_{w_{m,t}^u}^{w^{max}} F_{m,a}(x)dx \right). \tag{21}$$

As a result, the operational risk due to wind power accommodation can be directly estimated by (20)-(21).

Note that the above estimation method for the operational risk is conservative, because the worst pair of CDFs, i.e., $F_{m,a}$ and $F_{m,b}$, instead of the worst single CDF is employed. However, as shown in Fig. 2, when $F_{m,a}(w_{m,t}^u) > F_{m,b}(w_{m,t}^l)$, the operational risk estimated using the worst pair of CDFs is exactly equal to that estimated using the worst single CDF, since in this regard the worst single CDF can always be constructed by connecting the points $F_{m,b}(w_{m,t}^l)$ and $F_{m,a}(w_{m,t}^u)$ with a non-decreasing curve, such as the CDF a-b-c-d in the figure. Moreover, as will be illustrated in Section V, the more the available data, the narrower the CDF CBs, and thus the larger the probability of $F_{m,a}(w_{m,t}^u) > F_{m,b}(w_{m,t}^l)$. Therefore, the

above operational risk estimation method is suitable for wind power because wind power usually has a considerable amount of sample data in practice.

B. Linearization of the Operational Risk

Note that (20)-(21) are difficult to calculate due to their nonlinearity. Thus they are approximately linearized by using the piecewise linear approximation (PLA) method [32]. We take Eq. (20) for example to show how the risk components are linearized and how the piecewise linear approximation coefficients are obtained. The linearization procedure of Eq. (20) can be found as follows.

Step 1: The support of the random wind power x is divided equally to obtain break points $o_{m,t,s'}, s' = 1, 2, ..., S^l$. And then $w^l_{m,t}$ can be reformulated as:

$$\begin{cases} w^l_{m,t} = \sum\limits_{s'=1}^{S^l-1} w^l_{m,t,s'}, \\ \sum\limits_{s'=1}^{S^l-1} U^l_{m,t,s'} = 1, \\ o^l_{m,t,s'} U^l_{m,t,s'} \le w^l_{m,t,s'} \le o^l_{m,t,s'+1} U^l_{m,t,s'}, \end{cases} \tag{22}$$

where S^l is the number of break points; $U^l_{m,t,s'}$ is 0-1 variable indicating whether $w^l_{m,t}$ is located at segment $(s', s'+1)$; $w^l_{m,t,s'}$ is the value of $w^l_{m,t}$ in the segment $(s', s'+1)$.

Step 2: Let $F_{m,b}(o_{m,t,s'})$ be the cumulative probability corresponding to the break point $o_{m,t,s'}$. Then, we can obtain the corresponding operational risk components related to the load shedding $\max\limits_{P_m \in \mathcal{A}_m} \phi^{PS}_{m,t}$ when $w^l_{m,t} = o_{m,t,s'}$, as follows.

$$\max_{P_m \in \mathcal{A}_m} \phi^{PS}_{m,t} = \int_0^{o_{m,t,s'}} F_{m,b}(x)dx. \tag{23}$$

Step 3: The risk components related to the load shedding $\max\limits_{P_m \in \mathcal{A}_m} \phi^{PS}_{m,t}$ can be linearized as:

$$\max_{P_m \in \mathcal{A}_m} \phi^{PS}_{m,t} = \sum_{s'=1}^{S^l-1} (a^l_{m,t,s'} w^l_{m,t,s'} + b^l_{m,t,s'} U^l_{m,t,s'}) \tag{24}$$

where

$$\begin{aligned} a^l_{m,t,s'} &= \frac{F_b(o_{m,t,s'+1}) - F_b(o_{m,t,s'})}{o_{m,t,s'+1} - o_{m,t,s'}} \\ b^l_{m,t,s'} &= -\frac{F_b(o_{m,t,s'+1}) - F_b(o_{m,t,s'})}{o_{m,t,s'+1} - o_{m,t,s'}} o_{m,t,s'} \\ &\quad + \int_o^{o_{m,t,s'}} F_{m,b}(x)dx \end{aligned} \tag{25}$$

where (24) and (25) are the PLA of $\max\limits_{P_m \in \mathcal{A}_m} \phi^{PS}_{m,t}$; $a^l_{m,t,s'}$ and $b^l_{m,t,s'}$ are the piecewise linear approximation coefficients.

As a result, Eq. (20) can be linearized as Eqs. (22), (24), (25). Similarly, Eq. (21) can also be linearized using the same aforementioned procedure.

It should be noted that (22)-(25) reveal that to compute the operational risk using the PLA method, only the cumulative probabilities at the selected break points are required.

C. Deterministic Reformulation of Transmission Constraints

To eliminate the uncertain variables that exist only in the constraints of (17)-(18), Soyster's method is employed to equivalently reformulate (17)-(18) as deterministic constraints (26)-(27). More details can be found in [11].

$$\begin{cases} \sum\limits_{m \in \mathcal{M}} [(M_{ml} + \sum\limits_{i \in \mathcal{G}} M_{il}\alpha_{i,t})(\Delta p^{up}_{m,t}) + \lambda^{dn}_{ml,t}] \\ \ge -T_l - \sum\limits_{i \in \mathcal{G}} M_{il} p_{i,t} - \sum\limits_{m \in \mathcal{M}} M_{ml} p_{m,t} - \sum\limits_{j \in \mathcal{J}} M_{jl} d_{j,t} \\ \lambda^{dn}_{ml,t} \le -(M_{ml} + \sum\limits_{i \in \mathcal{G}} M_{il}\alpha_{i,t})(\Delta p^{up}_{m,t} + \Delta p^{dn}_{m,t}) \\ \lambda^{dn}_{ml,t} \le 0, \forall m, \forall l, \forall t \end{cases} \tag{26}$$

$$\begin{cases} \sum\limits_{m \in \mathcal{M}} [(M_{ml} + \sum\limits_{i \in \mathcal{G}} M_{il}\alpha_{i,t})(-\Delta p^{dn}_{m,t}) + \lambda^{up}_{ml,t}] \\ \le T_l - \sum\limits_{i \in \mathcal{G}} M_{il} p_{i,t} - \sum\limits_{m \in \mathcal{M}} M_{ml} p_{m,t} - \sum\limits_{j \in \mathcal{J}} M_{jl} d_{j,t} \\ \lambda^{up}_{ml,t} \ge (M_{ml} + \sum\limits_{i \in \mathcal{G}} M_{il}\alpha_{i,t})(\Delta p^{up}_{m,t} + \Delta p^{dn}_{m,t}) \\ \lambda^{up}_{ml,t} \ge 0, \forall m, \forall l, \forall t \end{cases} \tag{27}$$

D. The Sequential Convex Optimization Method for Bilinear Constraints

The resulting model forms a bilinear programming problem. To solve the problem, the sequential convex optimization method in [33] is applied to accommodate bilinear terms $\alpha_{i,t}\Delta p^{dn}_{m,t}$ and $\alpha_{i,t}\Delta p^{up}_{m,t}$ in constraints (11)-(12) and (26)-(27). In the method, two variables in bilinear terms are optimized in alternation, and then the original bilinear problem is solved by solving a sequence of linear problems. The specific procedures are as follows:

- **Step 1:** Let the iteration counter $N = 1$. Set the value of $\alpha^N_{i,t}$ according to the AGC unit capacity.
- **Step 2:** Substitute $\alpha_{i,t} = \alpha^N_{i,t}$ into the original bilinear problem. Solve the resulting linear problem, where $\Delta p^{dn}_{m,t}/\Delta p^{up}_{m,t}$ is the decision variable. And thus the optimal solution $\Delta p^{dn,N}_{m,t}/\Delta p^{up,N}_{m,t}$ is obtained.
- **Step 3:** Substitute $\Delta p^{dn}_{m,t}/\Delta p^{up}_{m,t} = \Delta p^{dn,N}_{m,t}/\Delta p^{up,N}_{m,t}$ into the original bilinear problem. Solve the resulting linear problem, where $\alpha_{i,t}$ is the decision variable. And thus the updated optimal solution $\alpha^{N+1}_{i,t}$ is obtained.
- **Step 4:** If $|\alpha^{N+1}_{i,t} - \alpha^N_{i,t}|/|\alpha^N_{i,t}| \le \beta$, where β is a predefined tolerance, then the final optimal solution is obtained, and the algorithm ends. Otherwise, let $N = N + 1$, and return to Step 2.

E. Fast Identification for Inactive Transmission Constraints

For large-scale power systems, there are too many complex transmission constraints that increase much computing burden. Fortunately, in practice, most of them are inactive. Therefore, the fast inactive constraint filtration method [34] is applied to reduce the model scale by ruling out the inactive transmission constraints. However, the method in [34] is originally used for the deterministic UC problem while the problem in this paper considers wind power uncertainty. To adapt the method to the problem in this paper, it is extended as follows.

Consider the following problems (ICF):

$$T_{l,t}^{max}(or\ T_{l,t}^{min}) = \max(or\ \min)\sum_{m\in\mathcal{M}} M_{ml}\tilde{p}_{m,t} + \sum_{i\in\mathcal{N}} M_{il}p_{i,t} + \sum_{m\in M}\sum_{i\in\mathcal{N}} M_{il}\alpha_{i,t}\Delta\tilde{p}_{m,t} + \sum_{j\in\mathcal{J}} M_{jl}d_{j,t}, \quad (28)$$

$$s.t. \quad \sum_{i\in\mathcal{N}}(p_{i,t}+\Delta\tilde{p}_{i,t}) + \sum_{m\in\mathcal{M}}\tilde{p}_{m,t} = D_t, \forall t, \quad (29)$$

$$0 \le p_{i,t} + \Delta\tilde{p}_{i,t} \le p_i^{max}, \forall i, \forall t. \quad (30)$$

It can be observed that the feasible sets of ICF are relaxations of the feasible set of the CI-DRED model. Thus, the optimal value of objective function (28) of the above minimization (maximization) optimization problem is a lower (upper) bound of the possible transmission line flow.

Moreover, according to the analysis in [34], the solution of ICF can be directly obtained without solving the optimization problem. Let $i_1, ..., i_e, ..., i_G$ be a permutation of $1, ..., e, ..., G$ such that $M_{i_1 l} \ge ... \ge M_{i_e l} \ge ... \ge M_{i_G l}$, and let an integer number k ($1 \le k \le G$) exist such that $\sum_{e=1}^{k-1} p_{i_e}^{max} \le D_t - \sum_{m=1}^{M}\tilde{p}_{m,t} \le \sum_{e=1}^{k} p_{i_e}^{max}$. Then

$$T_{l,t}^{max}(or\ T_{l,t}^{min}) = \sum_{e=1}^{k-1}(M_{i_e l} - M_{i_k l})p_{i_e}^{max} + \sum_{e=1}^{G}(M_{i_k l} - M_{i_e l})\tilde{p}_{m,t} + \sum_{j\in\mathcal{J}} M_{jl}d_{j,t}. \quad (31)$$

As shown in Eq. (31), the values of $T_{l,t}^{max}$ and $T_{l,t}^{min}$ depend on the realization of random variables $\tilde{p}_{m,t}$. Therefore, we can establish the following rules to quickly identify most of the inactive constraints in (26)-(27).

For any $l \in \mathcal{L}$ and $t \in \mathcal{T}$,

- If $\max_{0\le\tilde{p}_{m,t}\le w^{max}} T_{l,t}^{max} \le T_l$, constraint (27) is inactive;
- If $\min_{0\le\tilde{p}_{m,t}\le w^{max}} T_{l,t}^{min} \ge -T_l$, constraint (26) is inactive.

Note that the above rules are necessary conditions of inactive transmission constraints. In other words, not all inactive constraints can be identified based on the above rules while all identified inactive constraints are inactive for any realization of random variables $\tilde{p}_{m,t}$. By using this extended inactive constraint filtration method, the computation speed can be significantly improved.

V. Case Studies

Case studies on the modified IEEE 118-bus system and a real 445-bus system were conducted to illustrate the effectiveness of the proposed approach. All studies are implemented using GAMS 23.8.2 on a PC with an Intel Core i5-3470 3.2 GHz CPU and 8 GB RAM. The MILP solver is CPLEX 12.6. Unless otherwise specified, the confidence level γ is set to 0.95, the installed capacity of every wind farm is set to 50 MW, and prices for the wind power curtailment and load shedding are set to \$300/(MW·h) and \$3000/(MW·h) [35], respectively. In practice, the prices for wind power curtailment and loading shedding can be chosen according to historical data or long-term electricity contract. After solving each approach, monte carlo simulation with another 10^6 samples generated from the true probability distribution is employed to test the practical performance of each approach. The optimization results of each approach shown in Case Studies are the average of the practical performance of each approach.

TABLE I
Test Results Under Different CIs

	Sample Size	Size of ARWPs (MW)	Total cost (\$)	Risk cost (\$)
PW-CI	1000	1557.1	758908	7702
	5000	1498.3	757589	8070
	10^4	1451.6	757178	8526
	10^5	1419.4	756577	8880
FW-CI	1000	1635.2	760263	6795
	5000	1548.3	758350	7698
	10^4	1516.5	757841	7921
	10^5	1440.2	756894	8662

A. Modified IEEE 118-Bus System

The 118-bus system has 54 units and 186 lines. The generator capacity ranges from 20 MW to 650 MW, and 10 generators of 100 MW are selected as the AGC units. The system data can be found in [11], where the ramp rate of all AGC units is modified to 8 MW/h. Three wind farms are located at buses 17, 66, and 99, respectively. The forecasted wind power and total load in the test system are scaled down from the actual data of Eirgrid [36]. All uncertainties are assumed to originate from the wind power. Normal distribution is taken as the underlying true distribution of wind power and is employed to generate the realistic wind power forecasting error data. The standard deviation of wind power is set as 20% of the real value [37].

B. Comparing PW-CIs and FW-CIs

As mentioned in Section II.B, there are two kinds of CIs: 1) the PW-CIs, and 2) the FW-CIs. To compare the two kinds of CIs, simulations involving the different CIs are conducted on the 118-bus system. The test results can be found in Table I and Fig. 4.

From Table I, it is observed that as the sample size grows, the optimization results obtained using the PW-CIs and FW-CIs both become better and gradually approach to the optimization result obtained by the RED-PT. This occurs because the ambiguity sets constructed using the PW-CIs and FW-CIs shrink and the worst pairs of distributions in their established ambiguity sets both converge to the true distribution when more historical data are incorporated (See Fig. 4). On the other hand, Fig. 4 shows that, under the same sample size, the obtained FW-CIs are usually wider than the obtained PW-CIs. This illustrates the analysis in Section II.B that the FW-CIs usually lead to a more than required confidence level and cause a more conservative result.

C. Comparison with the Model Knowing the True Distribution

To illustrate the effects of considering the uncertainties of wind power distributions in the optimization, the proposed

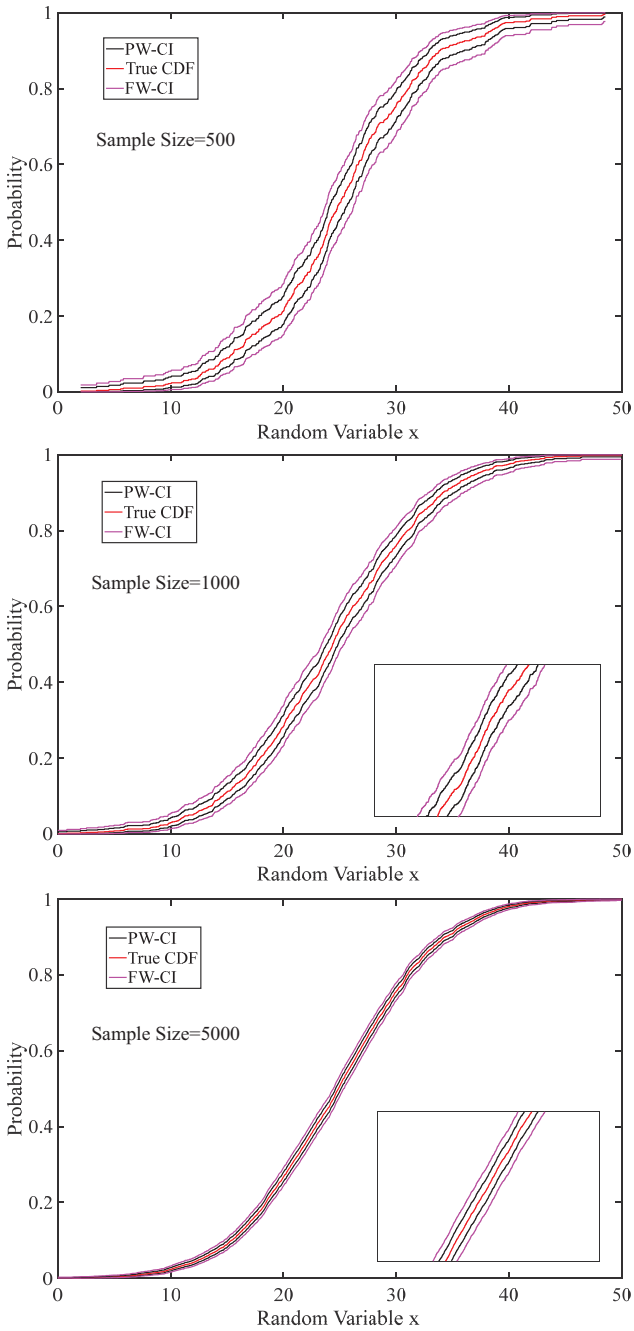

Fig. 4. Confidence bands under different sample sizes.

model is compared with the model assuming the true wind power distribution is exactly known. The test results are listed in Table II, where RED-PT represents the latter model and CI-DRED(n) denotes the proposed model with n samples.

From Table II, it is observed that as the sample size grows, the gap between the performances of CI-DRED and RED-PT decreases gradually. And it can be expected that if sufficient historical data are available, the gap may disappear and the optimization results will be almost the optimization results obtained under the true distribution. This indicates that the more the data, the less conservative the result obtained in CI-DRED. In other words, in CI-DRED, the conservativeness can be reduced by incorporating more historical data.

TABLE II
TEST RESULTS UNDER DIFFERENT APPROACHES

	Size of ARWPs (MW)	Total cost ($)	Risk cost ($)
CI-DRED (500)	1616.9	759563	7101
CI-DRED (1000)	1557.1	758908	7702
CI-DRED (5000)	1498.3	757589	8070
CI-DRED (10^4)	1451.6	757178	8526
CI-DRED (10^5)	1419.4	756577	8880
RED-PT	1386.7	756377	9249

On the other hand, the uncertainties of wind power distributions are considered in CI-DRED, and then the corresponding optimization result is obtained under the worst pair of distributions in the established ambiguity set. In contrast, the RED-PT knows the true distribution of wind power that is usually better than the worst pair of distributions in the ambiguity set. As a result, compared with the RED-PT, the CI-DRED obtains costly dispatch results regardless of the sample size. But note that as mentioned in Section II.A, the true distribution is hardly estimated precisely in practice.

In fact, the CBs for the wind power CDF represent the reliable information that can be extracted from the sample set. Fig. 4 shows the CBs for the wind power CDF under different historical sample data size. From Fig. 4, it can be observed that when few historical data are available, to ensure the required confidence level, the width of the CDF CBs should be relatively larger, i.e., the worst pair of distributions is much worse than the true distribution. In this case, more reserve should be required to ensure the robustness of the dispatch results, leading to a much higher total cost. On the contrary, when sufficient historical data are available, the CDF CBs will shrink to the true CDF and thus the worst pair of distributions in the ambiguity set will converge to the true distribution, as shown in Fig. 4. In this case, the best balance between the operational costs and risk can be obtained with precisely estimated wind power distribution.

It can also be observed that the risk cost increases with the sample number and the RED-PT has the highest risk cost. The opposite results can be found for the size of ARWPs. This is because the proposed approach aims to minimum the sum of the operational cost and the worst-case risk cost. Obviously, if the proposed approach and RED-PT have the same ARWP, their operational costs are the same while the worst-case risk cost of the proposed approach is larger than that of RED-PT. This is because the worst-case distribution instead of the true distribution is utilized in the proposed approach. Under the circumstances, to make a trade-off between the operational cost and the worst-case risk cost, the proposed approach has to enlarge the ARWP so that the operational cost will increase and the worst-case operational risk cost will decrease accordingly. In this case, the practical operational risk cost of the proposed approach will decrease and thus the practical operational risk cost of the proposed approach is less than that of RED-PT. Therefore, the RED-PT has the highest risk cost and the smallest ARWP. On the other hand, as the number of the samples is increasing, the worst-case distribution will

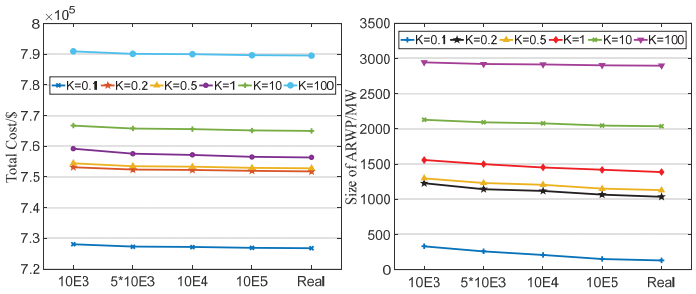

Fig. 5. Sensitivity Analysis of the Risk Cost Coefficients.

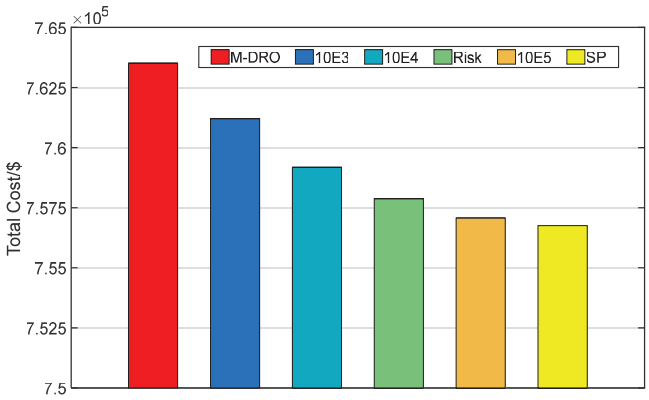

Fig. 6. Total cost under different approaches.

converge to the true distribution, as shown in Fig. 4. In other words, with the same ARWP, as the number of the samples is increasing, the worst-case operational risk cost will increase gradually. Therefore, larger ARWP will be obtained using the proposed approach with fewer samples so that the balance between the operational cost and the worst-case operational risk cost can be obtained. In the case, less practical operational risk cost and larger ARWP will be obtained using the proposed approach with fewer samples. Therefore, the practical risk cost increases with the sample number and the size of the ARWP decreases with the sample number.

D. Sensitivity Analysis of the Risk Cost Coefficients

Fig. 5 shows the total cost and the size of ARWPs under different risk cost coefficients, where 10E3, 5*10E3, 10E4, and 10E5 denote the proposed approach with 10E3, 5*10E3, 10E4, and 10E5 samples, respectively; "Real" denotes the proposed approach with the true distribution; K denotes the proportion of the tested risk cost coefficients and the originally set risk cost coefficients. It can be observed that as the size of the employed samples is increasing, the total cost will gradually decrease and the size of ARWPs will become smaller, regardless of the choice of the risk cost coefficients. In other words, although the choice of the risk cost coefficients affects the optimization solutions of the proposed approach, the choice of the risk cost coefficients will not change the conclusion, indicating the robustness of the conclusion of the risk cost coefficients.

TABLE III
RISK RELIABILITY UNDER DIFFERENT APPROACHES

Approach	10E3	10E4	10E5	M-DRO	Risk	SP
R-DRTD	97.7%	97.1%	96.2%	98.6%	89.6%	85.4%

E. Comparison with the Conventional Approaches

To illustrate the advantages of the proposed ambiguity set, the proposed approach is compared with SP, moment-based DRO, and the conventional risk-based approach. The conventional risk-based approach is chosen from [24], where the probability distribution is obtained using the maximum likelihood estimation. SP and the conventional risk-based approach assume the wind power follow the normal distribution. It should be point out that in this test, a real wind power sample data is employed, which is scaled down from the actual data of Eirgrid [36]. Fig. 6 shows the total cost of different approaches. The violation probability of the risk limit constraint for different approaches are further compared in Table III, where the required risk reliability level is set as 95%. In Fig. 6 and Table III, 10E3, 10E4, and 10E5 denote the proposed approach with 10E3, 10E4, and 10E5 samples, respectively; "Risk" denotes the conventional risk-based approach; M-DRO denotes the moment-based DRO. From Fig. 6, it can be observed that the total cost of the moment-based DRO is the highest whereas SP can obtain the lowest total cost. The proposed approach with different size of samples and the conventional risk-based approach are intermediates between the moment-based DRO and SP. From Table III, it can be observed that in SP and the conventional risk-based approach, the required risk reliability level cannot be guaranteed because the assumed probability distribution is not the true one. In contrast, the proposed approach can provide the risk reliability guarantee, regardless of the size of the employed samples, indicating the high risk reliability of the proposed ambiguity set.

F. Calculation Performance

To investigate the calculation performance of the proposed algorithm, the following two algorithms are compared.

BM-D: The algorithm in [13], which is based on the big-M method and the decomposition method. The big-M method is applied to handle bilinear constraints and the decomposition method is applied to release the computing burden resulting from transmission constraints.

SC-F: The algorithm presented in Section IV.

The calculation performance is demonstrated on the 118-bus system and the equivalent 445-bus system of Shandong Province, China. The 445-bus system has 48 units, 693 transmission lines and 5 integrated wind farms, and 15 units whose capacity ranges from 100 MW to 250 MW are selected as the AGC units. The test results are listed in Table IV.

Clearly, for both algorithms, the computational time changes little as the sample size grows, indicating that the computational efficiencies of both BM-D and SC-F are unrelated to the size of the employed historical data. Meanwhile, compared with the BM-D, the SC-F enhances the computational

TABLE IV
CALCULATION PERFORMANCE OF DIFFERENT APPROACHES

Approach	118-bus system		445-bus system	
	CPU time (s)	Total cost ($)	CPU time (s)	Total cost ($)
BM-D(1000)	12.364	758826	28.718	3066759
BM-D(5000)	13.152	757561	29.943	3063078
BM-D(10^4)	12.873	757162	28.429	3061948
BM-D(10^5)	12.581	756589	29.162	3060326
SC-F(1000)	7.875	758908	16.628	3066796
SC-F(5000)	8.498	757589	17.471	3063097
SC-F(10^4)	8.232	757178	17.611	3061887
SC-F(10^5)	7.930	756577	17.167	3060358

efficiency by 35.9% on average in the 118-bus system and 42.3% on average in the 445-bus system while maintaining the similar computational precision as BM-D, which illustrates the effectiveness of SC-F. In fact, the BM-D is slow because of the following reasons: 1) as mentioned in [13], the applied big-M method may face the scalability issue, especially for large-scale power systems because many auxiliary constraints and integer variables are introduced; 2) all transmission constraints will be checked in each iteration of the decomposition method, which will increase the computing burden. When the SC-F is employed, by identifying and eliminating most inactive transmission constraints (approximately 90% of the transmission constraints on both systems are identified as inactive and thus eliminated), the numbers of complex transmission constraints in the optimization is significantly reduced, and no integer auxiliary variables are introduced when applying the sequential convex optimization method rather than the big-M method. Thus, the computational efficiency of the SC-F can be increased significantly compared with the BM-D. In addition, the fast inactive constraint filtration method applied in the SC-F only eliminates the inactive transmission constraints that have no effect on the optimization result. Therefore, the computational precision can be maintained.

VI. CONCLUSIONS

In this paper, the DRO is integrated into real-time ED that considers the operational risk of accommodating wind power. Based on the imprecise probability theory, a CI-based wind power ambiguity set is directly constructed with wind power historical sample data. To achieve the operational risk reliability, the worst pair of CDFs in the proposed ambiguity set that can be identified directly is considered for the wind power accommodation risk assessment. As such, the CI-DRED model is formulated to strike a balance between the operational costs and risk regarding the uncertainties of wind power distributions. An efficient algorithm based on the sequential convex optimization method, and the fast inactive constraint filtration method is presented to improve the computational efficiency. Numerical results on the 118-bus and 445-bus systems reveal that the proposed ambiguity set shrinks to the true distribution as the amount of historical data increases. Therefore, the conservativeness of the solution can be reduced by incorporating more data. Compared with the regular RO and the moment-based DRO, the proposed approach can significantly reduces the conservativeness to obtain less conservative solutions. The proposed approach also outperformances SP and the conventional risk-based approaches in terms of the risk reliability. In addition, the scale of the optimization problem remains unchanged when using more data, ensuring the feasibility of incorporating more data to decrease the conservativeness. In conclusion, the proposed approach can efficiently model the uncertainty of probability distributions to strike a balance between the operational cost and risk while ensuring the risk reliability. Future works include developing a hourly day-ahead unit commitment model as well as incorporating the uncertainty of the line rating into the ambiguity set to establish distributionally robust methods which can simultaneously consider the uncertainties from different kinds of resources.

REFERENCES

[1] D. W. Ross and K. Sungkook, "Dynamic economic dispatch of generation," *IEEE Tran. Power App. Syst.*, vol. PAS-99, no. 6, pp. 2060–2068, Nov. 1980.

[2] B. H. Chowdhury and S. Rahman, "A review of recent advances in economic dispatch," *IEEE Tran. Power Syst.*, vol. 5, no. 4, pp. 1248–1259, Nov. 1990.

[3] H. Liang, Y. Liu, Y. Shen, F. Li, and Y. Man, "A hybrid bat algorithm for economic dispatch with random wind power," *IEEE Trans. Power Syst.*, vol. 33, no. 5, pp. 5052–5061, Sept. 2018.

[4] Y. Gu and L. Xie, "Stochastic look-ahead economic dispatch with variable generation resources," *IEEE Trans. Power Syst.*, vol. 32, no. 1, pp. 17–29, Jan. 2017.

[5] Y. Fu, M. Liu, and L. Li, "Multiobjective stochastic economic dispatch with variable wind generation using scenario-based decomposition and asynchronous block iteration," *IEEE Trans. Sustain. Energy*, vol. 7, no. 1, pp. 139–149, Jan. 2016.

[6] H. Gangammanavar, S. Sen, and V. M. Zavala, "Stochastic optimization of sub-hourly economic dispatch with wind energy," *IEEE Trans. Sustain. Energy*, vol. 31, no. 2, pp. 949–959, Mar. 2016.

[7] A. Ben-Tal and A. Nemirovski, "Robust solutions of linear programming problems contaminated with uncertain data," *Math. Program.*, vol. 30, no. 3, pp. 1337–1350, May. 2015.

[8] A. Ben-Tal and A. Nemirovski, "Robust convex optimization," *Math. Oper. Res.*, vol. 23, pp. 769–805, 1998.

[9] T. Zheng, J. Zhao, E. Litvinov, and F. Zhao, "Robust optimization and its application to power system operation," in *presented at 2012 CIGRE*, Paris, France, 2012.

[10] R. A. Jabr, "Adjustable robust opf with renewable energy sources," *IEEE Trans. Power Syst.*, vol. 28, no. 4, pp. 4742–4751, Nov. 2013.

[11] M. Yang, M. Q. Wang, F. L. Cheng, and W. J. Lee, "Robust economic dispatch considering automatic generation control with affine recourse process," *Electr. Power Energy Syst.*, vol. 81, pp. 289–298, Oct. 2016.

[12] A. Lorca and X. A. Sun, "Adaptive robust optimization with dynamic uncertainty sets for multi-period economic dispatch under significant wind," *IEEE Trans. Power Syst.*, vol. 30, no. 4, pp. 1702–1713, Oct. 2014.

[13] P. Li, D. Yu, M. Yang, and J. Wang, "Flexible look-ahead dispatch realized by robust optimization considering CVaR of wind power," *IEEE Trans. Power Syst.*, vol. PP, no. 99, pp. 1–1, 2018.

[14] Q. Bian, H. Xin, Z. Wang, and et. al, "Distributionally robust solution to the reserve scheduling problem with partial information of wind power," *IEEE Trans. Power Syst.*, vol. 30, no. 5, pp. 2822–2823, Sep. 2015.

[15] Z. Wang, Q. Bian, H. Xin, and D. Gan, "A distributionally robust coordinated reserve scheduling model considering cvar-based wind power reserve requirements," *IEEE Tran. Sustain. Energy*, vol. 7, no. 2, pp. 625–636, Apr. 2016.

[16] W. Wei, F. Liu, and S. Mei, "Distributionally robust co-optimization of energy and reserve dispatch," *IEEE Trans. Power Syst.*, vol. 7, no. 1, pp. 289–300, Jan. 2016.

[17] X. Lu, K. Chan, S. Xia, B. Zhou, and X. Luo, "Security-constrained multi-period economic dispatch with renewable energy utilizing distributionally robust optimization," *IEEE Tran. Sustain. Energy*, vol. 10, no. 2, pp. 768–779, Apr. 2019.

[18] Y. Chen, Q. Guo, H. Sun, Z. Li, W. Wu, and Z. Li, "A distributionally robust optimization model for unit commitment based on Kullback-Leibler divergence," *IEEE Tran. Power Syst.*, vol. 33, no. 5, pp. 5147–5160, Sept. 2018.

[19] C. Duan, W. Fang, L. Jiang, L. Yao, and J. Liu, "Distributionally robust chance-constrained approximate AC-OPF with wasserstein metric," *IEEE Tran. Power Syst.*, vol. PP, no. 99, pp. 1–1, 2018.
[20] L. Yao, X. Wang, C. Duan, J. Guo, X. Wu, and Y. Zhang, "Risk-based distributionally robust optimal power flow with dynamic line rating," *IET Gener. Transm. Distrib.*, vol. 12, no. 1, pp. 178–189, Oct. 2018.
[21] C. Wang, R. Gao, F. Qiu, J. Wang, and L. Xin, "Risk-based distributionally robust optimal power flow with dynamic line rating," *IEEE Tran. Power Syst.*, vol. PP, no. 99, pp. 1–1, 2018.
[22] P. Bhui and N. Senroy, "Robust optimal power flow with wind integration using Conditional Value-at-Risk," *Proc. of the 4th Intl. Conf. on Smart Grid Communications.*
[23] J. Wu, B. Zhang, W. Deng, and K. Zhang, "Application of Cost-CVaR model in determining optimal spinning reserve for wind power penetrated system," *Intl. Journal of Electrical Power Energy Syst.*, vol. 66, no. 1, pp. 110–115, Mar. 2015.
[24] N. Zhang, C. Kang, Q. Xia, Y. Ding, Y. Huang, R. Sun, H. J, and J. Bai, "A convex model of risk-based unit commitment for day-ahead market clearing considering wind power uncertainty," *IEEE Trans. Power Syst.*, vol. 30, no. 3, pp. 1582–1592, May 2015.
[25] C. Wang, F. Liu, J. Wang, F. Qiu, W. Wei, S. Mei, and S. Lei, "Robust risk-constrained unit commitment with large-scale wind generation: an adjustable uncertainty set approach," *IEEE Trans. Power Syst.*, vol. 32, no. 1, pp. 723–733, Jan. 2017.
[26] P. Walley, *Statistical Reasoning with Imprecise Probabilities*. Chapman & Hall, 1991.
[27] J. M. Bernard, "An introduction to the imprecise dirichlet model for multinomial data," *Int. J. Approx. Reason.*, vol. 39, no. 2, pp. 123–150, Jun. 2005.
[28] M. Yang, J. Wang, H. Diao, J. Qi, and X. Han, "Interval estimation for conditional failure rates of transmission lines with limited samples," *IEEE Trans. Smart Grid*, vol. 9, no. 4, pp. 2752–2763, Jul. 2018.
[29] P. Walley, "Inferences from multinomial data: Learning about a bag of marbles," *J. R. Stat. Soc. B.*, vol. 58, no. 1, pp. 3–57, Jan. 1996.
[30] M. Goldman and D. M. Kaplan, "Evenly sensitive ks-type inference on distributions," Tech. Rep., Working paper. [Online]. Available at: https://faculty.missouri.edu/ kaplandm/pdfs/GK2016 _dist_inf_KStype_longer.pdf 2015.
[31] P. Li, C. Wang, Q. Wu, and M. Yang, "Risk-based distributionally robust real-time dispatch considering voltage security," *IEEE Trans. Sustain. Energy*, vol. PP, no. 99, pp. 1–1, 2020.
[32] M. Q. Wang, H. B. Gooi, S. Chen, and S. Lu, "A mixed integer quadratic programming for dynamic economic dispatch with valve point effect," *IEEE Trans. Power Syst.*, vol. 29, no. 5, pp. 1–10, May. 2014.
[33] X. Chen, W. Wu, B. Zhang, and C. Lin, "Data-driven DG capacity assessment method for active distribution networks," *IEEE Trans. Power Syst.*, vol. 32, no. 5, pp. 3946–3957, Sep. 2017.
[34] Q. Zhai, X. Guan, J. Cheng, and H. Wu, "Fast identification of inactive security constraints in scuc problems," *IEEE Trans. Power Syst.*, vol. 25, no. 4, pp. 1946–1954, Nov. 2010.
[35] C. Wang, F. Liu, J. Wang, and S. Mei, "Risk-based admissibility assessment of wind generation integrated into a bulk power system," *IEEE Trans. Sustain. Energy*, vol. 7, no. 1, pp. 188–196, Oct. 2016.
[36] Wind power and load data. [Online]. Available: http://www.eirgridgroup.com/how-the-grid-works/system-information
[37] F. Bouffard and F. D. Galiana, "Stochastic security for operations planning with significant wind power generation," *IEEE Trans. Power Syst.*, vol. 23, no. 2, pp. 306–316, May. 2008.

Peng Li (Student Member, IEEE) received the B.S. degree in electrical engineering from the School of Electrical Engineering, Shandong University, Jinan, China, in 2015. He is currently pursuing the Ph.D. degree in the School of Electrical Engineering, Shandong University, Jinan, China. In 2018, he was a Visiting Ph.D Student with the Department of Electrical Engineering at Southern Methodist University, Dallas, Texas, USA, for five months. He was also a Visiting Ph.D Student with the Center for Electric Power and Energy, Department of Electrical Engineering, Technical University of Denmark, from July 2019 to January 2020.

His research interests include renewable energy integration and power system optimal operation.

Ming Yang (Senior Member, IEEE) received the B.Eng. and Ph.D degrees in electrical engineering from Shandong University, Jinan, China, in 2003 and 2009, respectively. He was an exchange Ph.D. student with Energy System Research Center, The University of Texas at Arlington, Arlington, TX, USA, from October 2006 to October 2007. He conducted Post-doctoral Research with the School of Mathematics of Shandong University from July 2009 to July 2011. From November 2015 to October 2016 he was a Visiting Scholar with the Energy Systems Division, Argonne National Laboratory, Argonne, IL, USA.

He is currently an Professor with Shandong University. He is an Associate Editor of the IEEE Transactions on Industry Applications and IET Renewable Power Generation. He is also an Editor of Protection and Control of Modern Power Systems. His research interests include power system optimal operation and control.

Qiuwei Wu (Senior Member, IEEE) received the Ph.D. degree in power system engineering from Nanyang Technological University, Singapore, in 2009. He was a Senior Research and Development Engineer with VESTAS Technology R&D Singapore Pte, Ltd., from March 2008 to October 2009. He has been an Assistant Professor with the Department of Electrical Engineering, Technical University of Denmark, Kongens Lyngby, Denmark, since 2009. In 2012, he was a Visiting Scholar with the Department of Industrial Engineering and Operations Research, University of California, Berkeley, for three months funded by Danish Agency for Science, Technology and Innovation, Denmark. He was a Visiting Scholar with the Harvard China Project, School of Engineering and Applied Sciences, Harvard University from 2017 to 2018.

His research interests include operation and control of power systems with high penetration of renewables, including wind power modeling and control, active distribution networks, and operation of integrated energy systems. He is the Deputy-Editor-in-Chief of the *International Journal of Electrical Power and Energy Systems*. He is an Editor of the IEEE Transactions on Smart Grid and IEEE Power Engineering Letters. He is the Regional Editor for Europe of the IET Renewable Power Generation, a Subject Editor of IET Generation, Transmission and Distribution and an Associate Editor of the *Journal of Modern Power Systems and Clean Energy*.